

Simulation of Blood Flow Coronary Artery with Consecutive Stenosis and Coronary-Coronary Bypass

Seyed Esmail Razavi*, Ramin Zانبوري, Omid Arjmandi-Tash

School of Mechanical Engineering, University of Tabriz, Tabriz, Iran

ARTICLE INFO

Article Type:
Research Article

Article History:
Received: 11 May 2011
Revised: 28 July 2011
Accepted: 31 July 2011
ePublished: 05 Aug 2011

Keywords:
Coronary Artery
Consecutive Stenosis
Newtonian Fluid
Anastomotic Vessel
Shear Stress
Navier-Stokes Equations
Stenose Possibility

ABSTRACT

Introduction: In this research the behavior of coronary arteries has been studied with symmetric and asymmetric consecutive stenosis, and grafted vessels. **Methods:** The incompressible Navier-Stokes and energy equations were discretized with second-order upwind method. Assumptions such as Newtonian fluid, wall rigidity and steady-flow were used. **Results:** All the calculations showed the same results with Newtonians and non-Newtonian fluids. It was found that the possibility of stenosis be reduced by increasing the graft angle. However, there exists further stenosis possibility. Among the three graft angles 20, 30° and 40, the 30° was found to be the reliable ones. **Conclusion:** Based on these findings, it can be deduced that there would be a high risk of further atherosclerosis when the first stenose has the maximum percentage.

Introduction

Heart diseases possess high importance and most of sudden deaths are caused by them. Sudden heart death is the direct cause of heart failure which may happen for many different reasons. The cause of sudden heart death increases severely by aging among natural sudden death reasons. In a group of 45-65 years old, sudden heart death among men was 7 times more than women. As engineering science was entered into the realm of medicine, a new horizon was opened in medical problem solving and made easy to diagnose and cure diseases. The atherosclerosis tissue pattern has a distinctive relation with flow pattern and the shear stress is imposed through blood to vessel wall. A number of studies show that stress and strain affect the biological activity of tissues. Low shear stress for example causes adhesion of white blood cells. Also, the oscillation and vertical stress inertia cause fracture and rupture of white blood cells toward internal vessels which provoke the blockage, formation and progress of blood clot in the vessel.

Some studies were carried out by Mann *et al.* on vessel blockage (Mann *et al.* 2002). Mann introduced the critical blockage in blood vessels and showed that only after 70% blockage in the vessel section, there will be considerable decrease in blood flow of vessels. Ko *et al.* numerically studied with bypass the effect of grafted angle on blood flow in vessel blockages (Ko *et al.* 2008). They raised their models by a 70% blockage and by hypotheses; they focused on grafted angles of 45°, 60° and 75°. Mustapha *et al.* proposed numerical simulation of blood flow in irregular vessel blockage (Mustapha *et al.* 2010). In their model, they hypothesized a part of a vessel in which there were two axial successive blockages having rough surface. Their model consisted of four successive blockages with percentages of (48%, 48%), (48%, 74%), (74%, 74%) and (74%, 48%). This study revealed that there are some differences between models of two irregular blockages, cosine, and long sine mono-blockage. In another study, Mustapha *et al.* investigated unsteady magnetohydrodynamic blood flow through irregular multi-stenosed arteries (Mustapha *et al.* 2009). Wei *et al.* carried out the numerical investigation

*Corresponding author: Seyed Esmail Razavi (PhD), Tel.: +98 411 3367914, Fax: +98 411 3367929, E-mail: razavi@tabrizu.ac.ir

of non-Newtonian flows in double blockages by irregular finite volume method (Wei *et al.* 2009). Their study was based on two dimensional incompressible and power-law non-Newtonian treatments. Their models included three successive blockages with percentages of (15%, 50%), (30%, 50%) and (50%, 50%). This study clarified that there are some differences between Newtonian and non-Newtonian treatments.

Vimmr *et al.* studied non-Newtonian effect of blood flow in femoral and coronary to coronary bypass (Vimmr *et al.* 2009). The three dimensional, Newtonian, non-Newtonian, and incompressible flow assumptions were used. They used hexahedral grids and solved Navier-Stokes' equations along with Carreau model. Prokop *et al.* solved the two and three dimensional Navier-Stokes equations for the Newtonian and non-Newtonian fluids in a bypass (Prokop *et al.* 2009). Their flow was also considered incompressible, steady and unsteady. The power-law was applied for non-Newtonian case. An investigation on the effects of stent geometry with different geometries on blood flow in 2D and 3D computational fluid dynamics models has already been reported (Dehlaghi *et al.* 2008). Blood velocity profiles and shear stress values were computed in three different sites and blood flow was assumed as a fully developed incompressible Newtonian flow and rigid boundary conditions were assumed for all models. The governing Navier–Stokes equations were solved using commercial software. It was shown that analyses of wall shear stress profile are essential in stent design between stent struts, and in pre-stent and post-stent regions. Additionally, it is shown that the wall shear stress increases markedly by application of a flow divider in stented segment.

Bashi Shahabi *et al.* performed the simulation of beating blood flow through non-Newtonian fluid in blocked vessels (Bashi Shahabi *et al.* 2003). Blocked vessel was of 75% blockage and the changes were investigated in flow field for 12.5 and 7.5 Womersely number. In another work, the regimes of blood flow were compared in aorta-coronary and coronary-coronary bypass (Ahmadluye Darab *et al.* 2009). The pulsative three dimensional blood flow was modelled for blockage of 50% by FLUENT software. The homogeneous Newtonian blood and blockage were studied. It was revealed the lack of recirculation zone, low shear stress in coronary-coronary bypass against aorta-coronary and highness of temporal and spatial oscillation of shear stress in aorta-coronary bypass in comparison to coronary-coronary. The effect of grafted angles was investigated in ref on time oscillation of shear stress in aorta-coronary and coronary-coronary bypasses (Ahmad luye Darab *et al.* 2007). In this study, it was assumed the pulsatile, blood flow, Newtonian, homogeneousness, blockage of coronary vessels, graft and laminar flow.

Bypasses are considered with grafted angles of 20°, 30° and 40° on blockage percent of 75%. It was found that high blockage potential would be produced in coronary-coronary bypass and it was proposed the grafted angles lower than 30°. The unsteady non-Newtonian simulation of blood has already been studied in three dimensional geometry of vessel with thorough bypass (Zohravi *et al.* 2009). The Carreau model was used for non-Newtonian fluid. Velocity distribution, shear stress of walls under different conditions, blockage of 100% and 56%, sever decrease of blood flow and above shear stress in blockage were represented.

The blood flow was solved in coronary vessels with successive blockages (Ebadi *et al.* 2005), in which three sinusoidal successive blockages were assumed with two different percentages of 84% and 70% and rigid vessels. It was found that increasing shear stress and decreasing normal stress became sever by growing the blockage rate. These changes are much more severe when the discharge of blood flow is in its maximum rate. Investigations show that there are no vertical flows at the back of blockage due to the low Reynolds' number. In this paper our aim is to simulate the different models of vessels with various successive blockages in order to clarify the effective causes in re-blockages after vessel graft.

Methods

Governing equations

The Navier-Stokes equations of Newtonian flow consists of the following:

$$\nabla \cdot \mathbf{V} = 0 \quad (1)$$

$$\rho \frac{D\mathbf{V}}{Dt} = -\nabla \cdot \mathbf{P} + \nabla \cdot (\mu \nabla \mathbf{V}) \quad (2)$$

Solution algorithm consists of implicit SIMPLE in segregated form. Under Relaxation factor for pressure and momentum were 0.3 and 0.7 respectively. The convergence criteria was set to 10^{-6} for Newtonian case. For convective fluxes, the second-order upwind is used for all the equations. The convergence is achieved in iteration steps ranging from 115 to 130.

Boundary conditions and assumptions

Newtonian flow is analyzed between systolic and diastolic pressures. The systolic and diastolic velocities are consisted of 0.3, 0.2, 0.12, 0.06 and 0.045 (Takei *et al.* 2010, Kern *et al.* 2002, Yamamoto *et al.* 2002, Dimitrow *et al.* 2000). In velocity of systole (i.e. 0.2), Reynolds' number is 240 with the viscosity of 0.0035 Pa/s, density of 1050 Kg/m³ and diameter of coronary vessel of 4mm. The wall is assumed rigid because of minor effects of vessel elasticity. Also, the coronary

vessels have to transfer blood to heart muscle between systole, diastole, and rest time of heart. Therefore, blood flow can be assumed steady in coronary. For this reason coronary vessels are less affected by heart oscillations like aorta. Also the effect of entrance length was considered in the form of additional vessel length. Boundary conditions are described as velocity at inlet and as pressure at outlet. Inlet flow velocity is equal to 0.2 m/s and external pressure boundary condition is assumed zero at the end of vessel. Also, no-slip boundary condition is considered at vessel wall. Blood specific heat is 3850 J/Kg.k In energy equation and thermal conductivity is 0.5 W/m.k.

Geometric characteristics and grid

Based on the ref (Mann *et al.* 2002, Ko *et al.* 2008) three tufts of vessels with successive blockage of 70% symmetric, 80% one-way; 75% symmetric, 75% one-way; 80% symmetric, 70% one-sided having bypasses with main diameter of 4mm and minor diameter of 3mm are chosen and modeled in three dimensional form. Symmetric blockage broadness was 10 mm, one-way blockage 15 mm and vessel graft angle was changing from 20° to 40°. Sample models are shown in Figs. 1 and 2.



Fig. 1. Vessel model with successive blockages of 70% and one-sided of 80%.



Fig. 2. Vessel model with successive blockages of 70% symmetric and 80% one- sided with graft angle of 30°.

Due to geometrical complexity, unstructured triangular grids are used. In Fig. 3, a part of grid is shown.

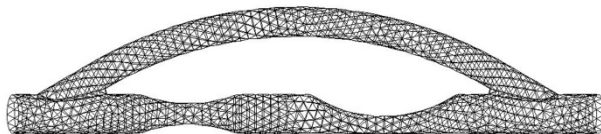


Fig. 3. Three dimensional unstructured grid with successive blockage of 70% symmetric and 80% one- sided with graft angle of 30° generated with unstructured triangular elements.

Results and discussion

According to Figs. 4 to 6 of shear stress distribution it can be concluded that as graft angle increases the shear stress enlarges in main vessel and the possibility of re-blockage reduces at the beginning and end of grafted vessel. Increasing the graft angle lowers the shear stress in grafted vessel and the possibility of re-blockage goes up. This can be considered for shear stress in Figs. 4 to 6.

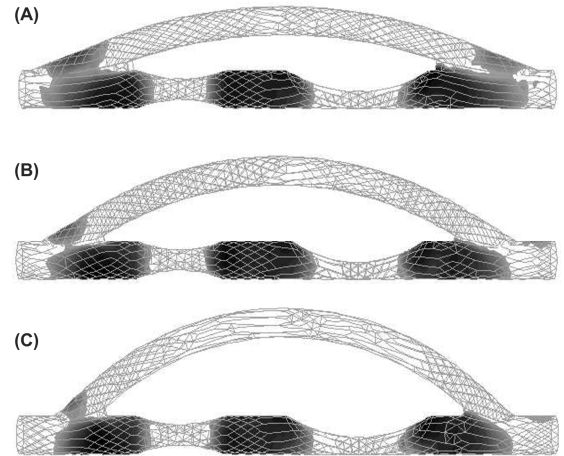


Fig. 4. Shear stress distribution at Re=240 for vessel with successive blockages of 70% symmetric and 80% one-sided with: A) graft angle 20°, B) graft angle 30°, C) graft angle 40°.

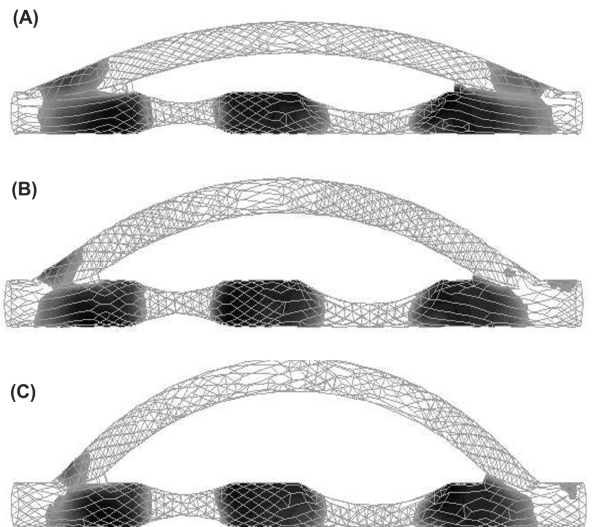


Fig. 5. Shear stress distribution at Re=240 for vessel with successive blockages of 75% symmetric and 75% one-sided with: A) graft angle 20°, B) graft angle 30°, C) graft angle 40°.

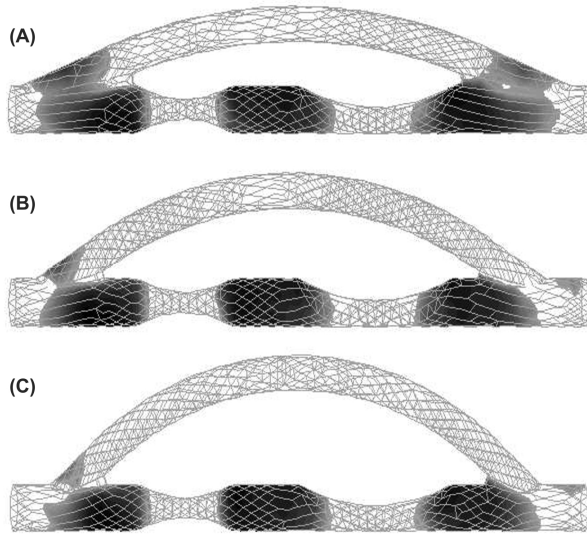


Fig. 6. Shear stress distribution at $Re=240$ for vessel with successive blockages of 80% symmetric and 70% one-sided with: A) graft angle 20° , B) graft angle 30° , C) graft angle 40° .

By considering these figures, maximum spots and its neighbors, it can be seen that as graft angle increases shear stress in main vessel is intensified which leads to possible diminishing of re-blockage. According to shear stress graph, if an average line is assumed it will be seen that as the graft angle increases this line is descending. Hence, the shear stress is decreased and the possibility of re-blockage will be amplified. For more comparison of models, minimum and average shear stresses are shown in Table 1.

Justification of this problem through pressure is depicted in Figs. 7 to 9 which are somewhat different from other ones. Main vessel pressure is sinusoidal and as graft angle increases it moves downward gradually. Through the length of main vessel the decrease of pressure reduces the chance of re-blockage. The graft vessel pressure is an inclined line. As the graft angle increases the inclination of this line goes up which in turn leads to decrease of shear stress thereby producing the blockage.

Table 1. Minimum and average shear stress for analyzed models

	80% symmetric, 70% one-sided		75% symmetric, 75% one-sided		70% symmetric, 80% one-sided	
	τ_{avg} (Pascal)	τ_{min} (Pascal)	τ_{avg} (Pascal)	τ_{min} (Pascal)	τ_{avg} (Pascal)	τ_{min} (Pascal)
Main Vessel without Bypass	1.178×10^{-2}	2.877×10^{-3}	1.121×10^{-2}	3.135×10^{-3}	1.167×10^{-2}	3.735×10^{-3}
Main Vessel with graft angle 20°	7.782×10^{-3}	2.025×10^{-3}	7.805×10^{-3}	1.966×10^{-3}	7.815×10^{-3}	1.801×10^{-3}
Bypass Vessel with graft angle 20°	1.036×10^{-2}	2.134×10^{-3}	9.024×10^{-2}	2.362×10^{-3}	1.056×10^{-2}	1.801×10^{-3}
Main Vessel with graft angle 30°	7.803×10^{-3}	1.831×10^{-3}	8.041×10^{-3}	2.167×10^{-3}	7.990×10^{-3}	1.815×10^{-3}
Bypass Vessel with graft angle 30°	1.086×10^{-2}	4.112×10^{-3}	1.011×10^{-2}	4.003×10^{-3}	1.054×10^{-2}	4.051×10^{-3}
Main Vessel with graft angle 40°	7.885×10^{-3}	1.794×10^{-3}	8.053×10^{-3}	1.883×10^{-3}	8.121×10^{-3}	1.822×10^{-3}
Bypass Vessel with graft angle 40°	1.057×10^{-2}	2.754×10^{-3}	9.821×10^{-3}	3.007×10^{-3}	1.037×10^{-2}	2.804×10^{-3}

Conclusion

Overall, it can be concluded that among graft angles, 30° is the most ideal one. It can be justified that 20° reduces the flow velocity at graft vessel inlet and outlet because of the broadness of graft section and its neighbor blockage. Then the shear stress falls down and the possibility of re-blockage will be increased. But in 30° and 40° , as angle increases the graft section shrinks and there will be a kind of disturbance at vessel inlet and outlet which leads to the rise of velocity and shear stress in that place and the possibility of re-blockage is lessened.

The important point is that even though if the graft angle grows, the possibility of re-blockage in graft vessel inlet and outlet will be decreased. The shear stress decreases in the grafted vessel and the possibility of re-blockage is amplified. Due to the possible re-blockage rise at 20° in comparison to other angles, it will be abandoned but 30° and 40° are similar to each others.

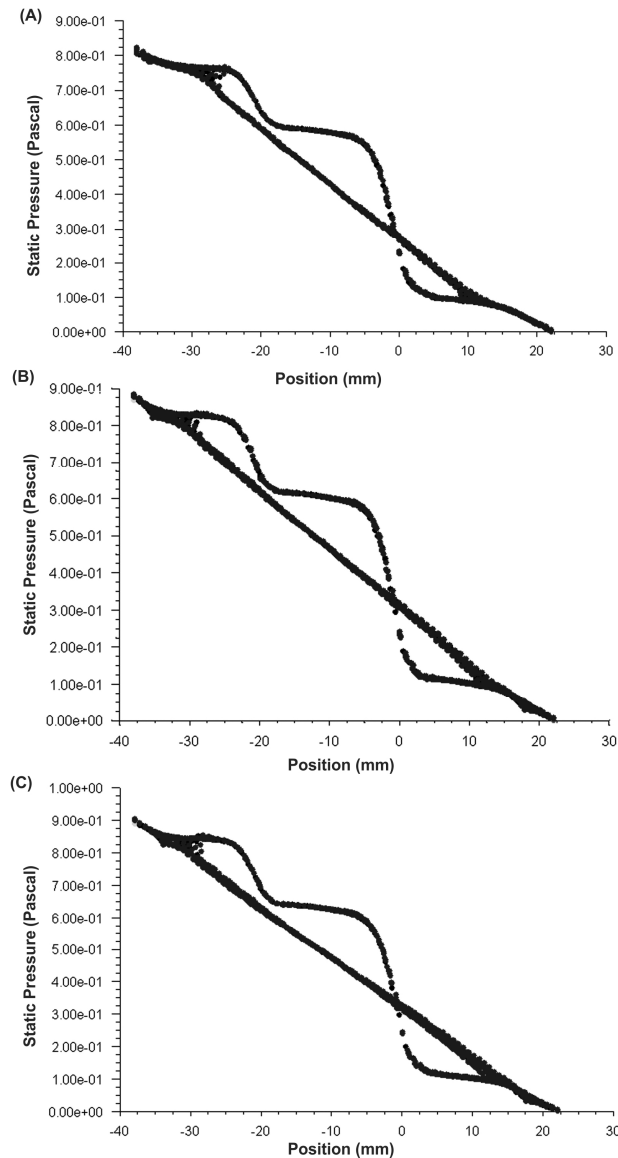


Fig. 7. Pressure variations at $Re=240$ for main and bypass vessel with successive blockages of 70% symmetric and 80% one- sided with: A) graft angle 20° , B) graft angle 30° , C) graft angle 40° .

In order to choose the most suitable angle, we compare the total shear stress within the grafted vessel and main vessel inlet and outlet points of grafted vessel. The shear stress extent will be gathered from place to place. The leading result is that the total shear stress at 30° is more than 40° so, among 20° , 30° and 40° , the most suitable one is 30° for vessel graft. The important point is that the maximum re-blockage possibility will occur in a state in which the first blockage has the maximum percentage against vessel inward flow i.e. a class of models that their first blockage is of high percentage, have the high risk of re-blockage in comparison to their symmetric counterparts.

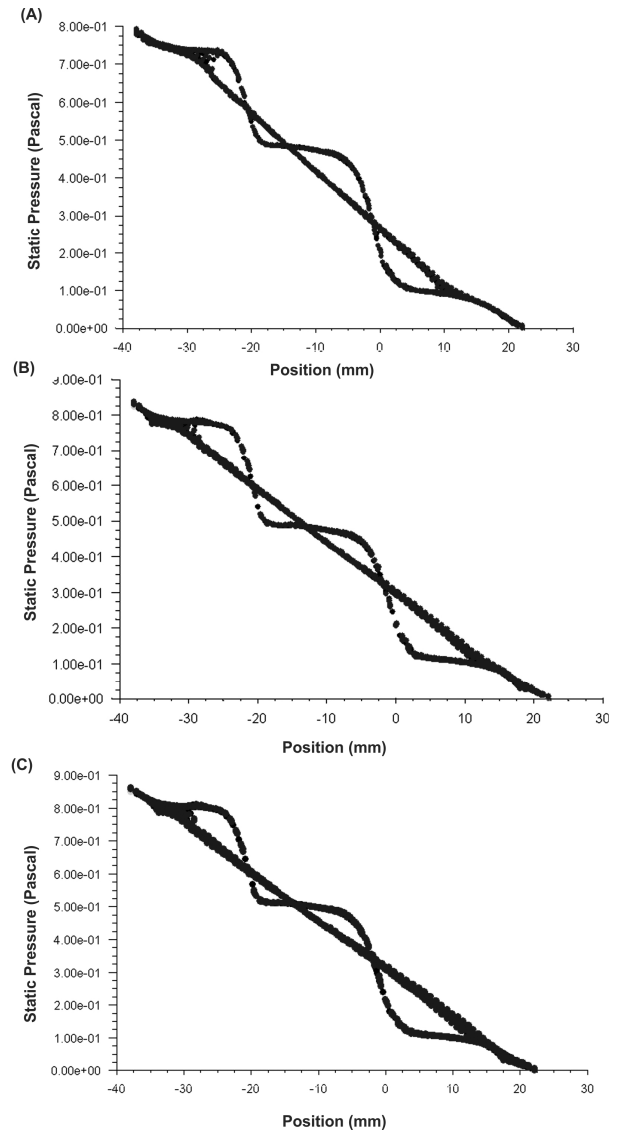


Fig. 8. Pressure variations at $Re=240$ for main and bypass vessel with successive blockages of 75% symmetric and 75% one- sided with: a) graft angle 20° b) graft angle 30° c) graft angle 40° .

Ethical issues

None to be declared.

Conflict of interests

The authors declare no conflict of interests.

Acknowledgement

Authors are thankful to the Tabriz University for its financial support.

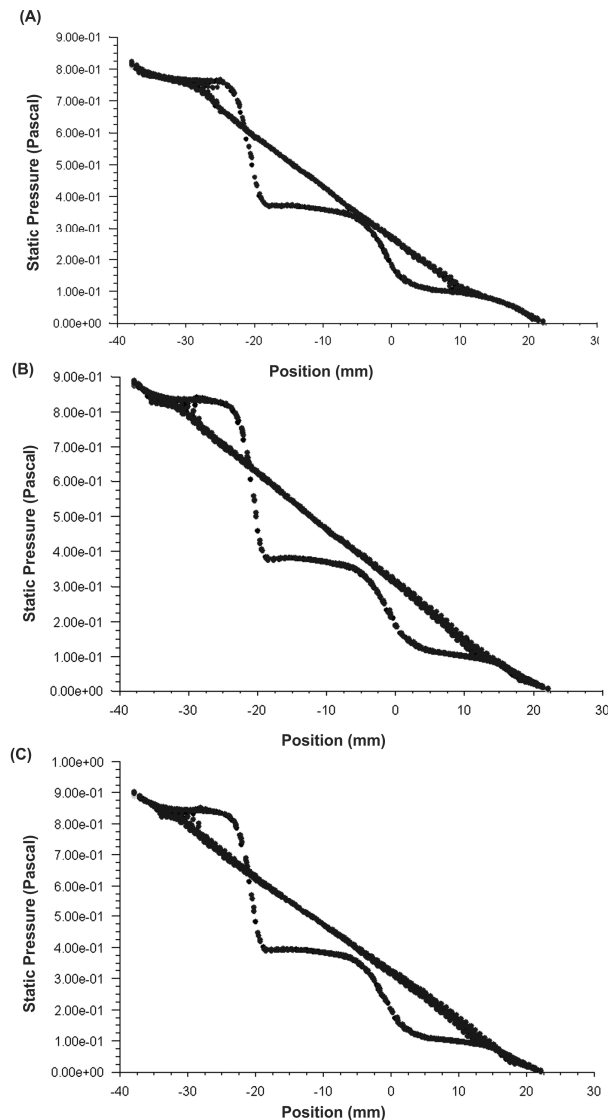


Fig. 9. Pressure variations at $Re=240$ for main and bypass vessel with successive blockages of 80% symmetric and 70% one-sided with: a) graft angle 20° b) graft angle 30° c) graft angle 40° .

References

- Mann R, Zhuang L, Lu X, Wang W, **2002**. Breaking Symmetry in Non-Planar Bifurcation: Distribution of Flow and Wallshear Stress. *Biorheology*, 39, 431-436.
- Ko T, Ting K, Yeh H, **2008**. A Numerical Study on the Effects of Anastomotic Angle on the Flow Fields in a Stenosed Artery with a Complete Bypass Graft. *International Communications in Heat and Mass Transfer*, 35, 1360-1367.
- Norzieha M, KumarMandal P, Johnston P, Amin N, **2010**. A Numerical Simulation of Unsteady Blood Flow through Multi-irregular Arterial Stenoses, *Applied Mathematical Modelling*, 34, 1559-1573.
- Mustapha M, Amin N, Chakravarty S, KumarMandal P, **2009**. Unsteady Magnetohydrodynamic Blood Flow through irregular

Multi-Stenosed Arteries. *Computers in Biology and Medicine*, 39, 896 – 906.

Wei G, Ru-xun L, Ya-li D, **2009**. Numerical Investigation on Non-Newtonian Flows Trought Double Constrictions By an Unstructured Finit Volume Method. *Journal of Hydrodynamics*, 21, 622-632.

Vimmr J, Jonářová A, **2009**. Non-Newtonian Effects of Blood Flow in Complete Coronary and Femoral Bypasses. *Mathematics and Computers in Simulation*, xxx , xxx-xxx.

Prokop V, Kozel K, **2009**. Numerical Simulation of Newtonian and Nnon-Newtonian Flows in Bypass, *Mathematics and Computers in Simulation*, xxx , xxx-xxx.

Dehlaghi V, Tafazoli Shadpoor M, Najarian S, **2008**. Analysis of wall shear stress in stented coronary artery using 3D computational fluid dynamics modeling, *Journal of materials processing technology*, 197, 174-181.

Ahmad Luye Darab M, Qalichi F, Ramezani A, **2009**. The Comparison of Blood Current Regimes in Aorta-Coronary and Coronary-Coronary Bypasses. 11th Medical Engineering Conference, Iran.

Ahmad Luye Darab M, Ramezani A, Qalichi F, **2007**. Investigated the effect of grafted angles on time oscillation of shear stress in aorta-coronary and coronary-coronary bypasses. 10th Chemical Engineering Conference, Iran.

Bashi Shahabi P, Modares Razavi M, **2003**. The Simulation of Blood Beating Current in Blocked Vessels through Non-Newtonian Fluid. 8th Fluids Dynamic Conference, Iran ,Tabriz University.

Ebadi A, Qalichi F, **2005**. Numeric Simulation of Blood Current in Coronary Vessels with Successive Blockages. 10th Iran National Congress of Chemistry Engineering, Iran, Sistan-Baluchestan University.

Zohravi E, Shirani E, Sadeghi M. **2009**. Inconsistent and Non-Newtonian Numeric Investigation of Blood in Three Dimensional Geometry of Vessel with Thorough Bypass. 12th Fluids Dynamic Conference, Babol, Industrial University of Nushirvan.

Takei Y, Tanaka N, Takahashi N, Kurohane S, Kijima H, Saruhara H, et al, **2010**. Clinical significance of coronary flow velocity measurement using transthoracic Doppler echocardiography for unstable angina: a two-case report. *Japanese Society of Echocardiography*, DOI 10.1007/s12574-010-0066-5.

Kern M, **2002**. The value of systolic flow velocity acceleration after PCI. *European Heart Journal*, 23, 1801-1802.

Yamamoto K, Iwakura K, Ikushima M, Masuyama T, Ogihara T, Fujii K, **2002**. Two different coronary blood flow velocity patterns in thrombolysis in myocardial infarction flow grade 2 in acute myocardial infarction. *journal of the American College of Cardiology*, 40(10), 1755-1760.

Dimitrow P, Krzanowski M, Nizankowski R, Szczeklik A, Dubiel J, **2000**. Effect of verapamil on systolic and diastolic coronary blood flow velocity in asymptomatic and mildly symptomatic patients with hypertrophic cardiomyopathy. *heart*, 83(3):262-6.